Proceedings of 20th International Congress on Acoustics, ICA 2010

23-27 August 2010, Sydney, Australia

A simple pinna model for generating head-related transfer functions in the median plane

Hironori Takemoto (1), Parham Mokhtari (1), Hiroaki Kato (1), Ryouichi Nishimura (1), and Kazuhiro Iida (2)

(1) National Institute of Information and Communications Technology (NICT),
2-2-2, Hikaridai, Seika-cho, Soraku-gun, Kyoto, 619-0288, Japan
(2) Chiba Institute of Technology,2-17-1, Tsudanuma, Narashino, Chiba, 275-0016, Japan

PACS: 43.64.Bt, 43.64.Ha

ABSTRACT

There is a common peak-notch pattern in head-related transfer functions (HRTFs) for the median plane, and the pattern provides cues for perceiving the elevation of the sound source. In the present study, to examine morphological features necessary for generating the typical peak-notch pattern, the pinna was modeled as a rectangular plate with a rectangular hole, and then it was modified to generate the pattern. The finite-difference time-domain method was used for calculating HRTFs by numerical simulation. The results of calculations indicated that the first peak was caused by the first closed-open resonance in the medio-lateral direction. On the other hand, the second and third peaks were caused by the first and second closed-closed resonances in the supero-inferior direction, which were also associated with the first notch. These findings implied that the vertical length and geometry of the hole mainly contributed to generating the typical peak-notch pattern, while the depth of the hole determined the first peak frequency.

INTRODUCTION

We have calculated head-related transfer functions (HRTFs) in the median plane from the head shape data measured by magnetic resonance imaging (MRI) using a finite-difference time-domain (FDTD) method [1-3]. Based on analyses of HRTFs among two males and two females, a common peak-notch pattern of HRTFs in the median plane was found. Figure 1 (a) shows HRTFs calculated from the segmented left pinna for a female and (b) schematically represents the typical peak-notch pattern. Three peaks (P1, P2, and P3) existed below 10 kHz and the first notch (N1) surrounded them. P1 constantly appeared across elevation angles, while P2 and P3 appeared at a relatively narrow range of angles centered at approximately 120˚. The frequencies of P1, P2, and P3 were stable, while the frequency of N1 systematically changed with elevation angle. The frequency of N1 was lower than that of P2 below 0˚, it increased as the elevation angle approached 120˚, and then it decreased to be lower than that of P2 above 180˚. According to Iida *et al.* [4], the trajectory pattern of the second notch (N2) is similar to that of N1 but at a higher frequency. However, an N2 pattern was not clearly observed in our simulations [1-3]. The trajectories of N1 and N2 and the stable P1 provide cues for localizing the elevation angle of the sound source [4].

We have also examined how peaks and notches of HRTFs in the median plane were generated based on simulations with an MRI measured pinna [3]. As a result, we arrived at the following conclusions:

(1) Although diffraction effects of the head on HRTFs were observed below 5 kHz, they were relatively small. Thus, the basic peak-notch pattern was maintained, even if HRTFs were calculated only from the pinna segmented from the head.

(2) One, two and three pressure anti-nodes were observed on the pinna cavities (concha, cymba, triangular fossa, and scaphoid fossa, as shown in Fig. 2) at P1, P2, and P3 frequencies, respectively. In all cases, one of these anti-nodes developed at the concha.

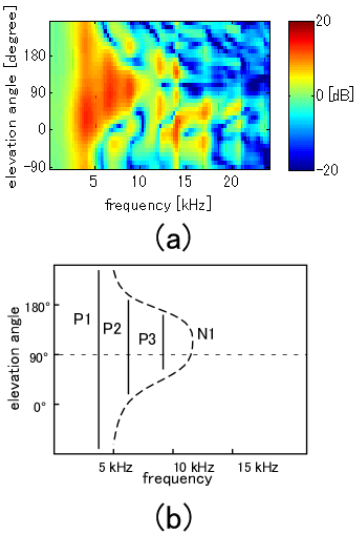

Figure 1. (a) HRTFs calculated from the segmented left pinna for a female in the median plane. (b) Schematic representation of typical peak-notch pattern.

(3) N1 is generated by the cancelation between the resonance of pinna cavities other than the concha (i.e., a resonance of the upper cavities, as shown in Fig. 2) and the incoming wave.

Although we qualitatively clarified how peaks and notches were generated, we could not reveal the relationship between morphological features of the pinna and frequencies of peaks and notches. This is because the pinna shape is too complex to define how to measure each cavity's shape such as depth and length. Thus, in the present study, we try to develop a simple pinna model which can generate the typical peak-notch pattern as shown in Fig. 1 (b) and examine morphologically essential features for the pattern.

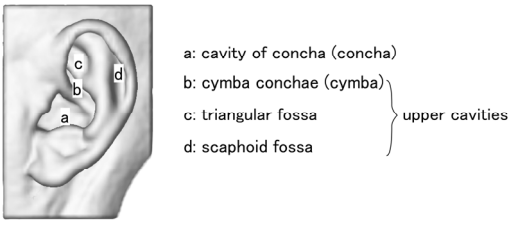

Figure 2. Anatomical part names of the pinna cavities

MATERIALS AND METHODS

Primitive model and HRTF calculation

Figure 3 (a) shows the simplest pinna model, which is a rectangular plate (72 mm height, 36 mm width, and 17 mm depth) with a rectangular hole (33 mm height, 16 mm width, and 15 mm depth). This model represents the left pinna, and the hole represents the pinna cavities. Hereafter this model is called the "primitive model." Note that the hole is long in the vertical direction, while the long axis of the real pinna cavities is tilted at approximately 30˚ backward.

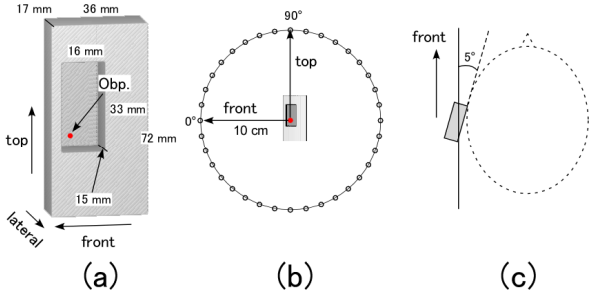

Figure 3. (a) Configuration of the "primitive model" (left pinna). Obp stands for the observation point. (b) Lateral view of simulation field and the elevation angle. (c) Top view of the simulation field and the tilt angle. The dashed line indicates the head.

The observation point (denoted by Obp. in Fig. 3 (a)) was placed at 1 mm lateral to the cavity's medial wall, 5 mm posterior to the cavity's frontal wall, and 6 mm superior to the cavity's bottom wall. This point corresponded to the entrance of the ear canal. A Gaussian pulse was fed to this point and the pressure change was calculated by the FDTD method [5,6] during 8 ms at points placed on the circumference of a circle with a radius of 0.1 m at 10 degree intervals (Fig. 3 (b)). Utilizing the reciprocity theorem, HRTFs up to 24 kHz were computed from pressure changes at those 36 points.

In the human body, the lateral surface of the pinna faces slightly forward. To incorporate this morphological feature, the pinna model was tilted at 5˚ to the medial plane (Fig. 3 (c)). Note that the elevation angle for the frontal direction was set at 0˚ and that for the overhead direction at 90˚.

Modification of primitive model

The "primitive model" was modified to examine effects of the morphological features on HRTFs and to generate the typical peak-notch pattern. Four types of modification were carried out and HRTFs were calculated after each modification. Note that the width of the rectangular cavity (antero-posterior dimension) was unmodified.

Modification 1: for examining effects of the cavity height on HRTFs. The height of the cavity (supero-inferior dimension) was reduced to 2/3 or 1/3. Hereafter, they are referred to as the "2/3 height model" and "1/3 height model," respectively (Fig. 4 (a) and (b)).

Modification 2: for examing effects of the location of the observation point on HRTFs. The cavity was shifted downward in order to place the observation point at 1/3 or 1/2 the height of the cavity. Note that the cavity size was unchanged. They are referred to as the "1/3 position model" and "1/2 position model," respectively (Fig. 4 (c) and (d)).

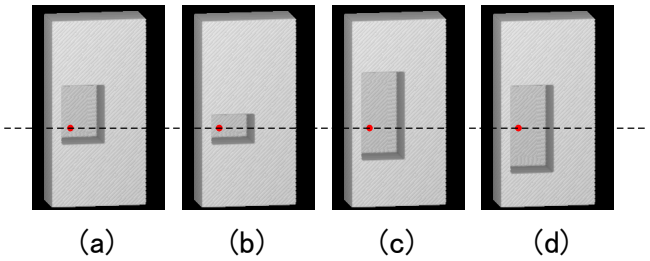

Figure 4. (a) "2/3 height model." (b) "1/3 height model." (c) "1/3 position model." (d) "1/2 position model." The observation point (denoted by the red circle) was fixed to the pinna as indicated by the dashed line.

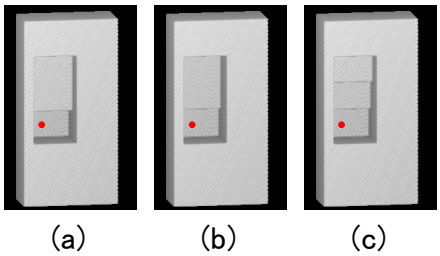

Figure 5. (a) "8 mm two-step model." (b) "4 mm two-step model." (c) "three-step model." The observation point is denoted by the red circle.

Modification 3: for examining effects of a two-step cavity on HRTFs. To increase the complexity of the cavity, a step was added. The depth of the upper 2/3 of the cavity was reduced by 8 mm and 4 mm. They are referred to as the "8 mm two-step model" and "4 mm two-step model," respectively (Fig. 5 (a) and (b)).

Modification 4: for examining effects of a three-step cavity on HRTFs. The depth of the upper 1/3 of the cavity was reduced by 8 mm, and that of the middle 1/3 was reduced by 4 mm. This model is referred to as the "three-step model" (Fig. 5 (c)).

Pressure distribution pattern

In order to examine acoustic phenomena at frequencies of peaks or notches, the time course of the instantaneous pressure distribution pattern was calculated. For a given elevation angle and at a given frequency, the analysis field was excited by a sinusoidal wave at that frequency. Depending on the elevation angle, the source point was selected from among the 36 points used for HRTF calculation. After reaching a

steady-state, the pressure distribution pattern within the whole analysis field was recorded at a 200 kHz sampling rate during 0.5 ms. The pressure distribution pattern at each sampling step was visualized by a volume rendering technique.

RESULTS AND DISCUSSION

HRTFs and pressure distribution pattern for "primitive model"

Figure 6 represents HRTFs calculated from the "primitive model." Below 15 kHz, five peaks (3.5 kHz, 6.75 kHz, 11.25 kHz, 11.75 kHz, and 13 kHz) were observed. Between the first and second peaks, a notch was observed below 0˚ and above 180˚. The frequency of this notch gradually increased as the elevation angle approached 0˚ from below. From 0˚ to 180˚, the notch trajectory was not clearly observed. Above 180˚, the notch frequency decreased as the elevation angle increased. At 0˚ and 180˚, the notch frequency agreed with the second peak's frequency, and thus, they appeared to cancel each other. Except for elevation angles from 0˚ to 180˚, the notch pattern resembled a typical N1 trajectory.

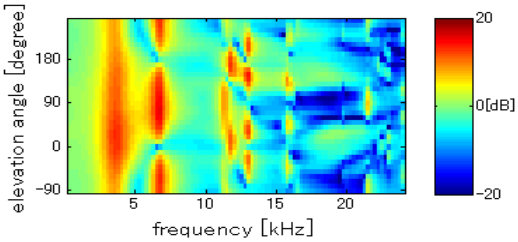

Figure 6. HRTFs for "primitive model."

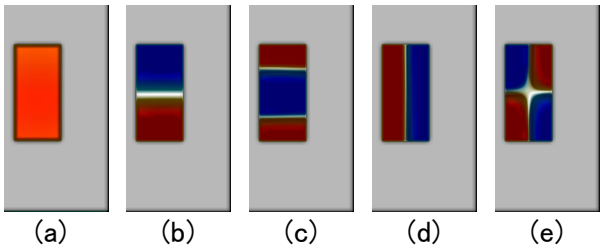

Figure 7. Pressure distribution patterns at the lower five peaks of the "primitive model." The excited frequency and source elevation angle for each peak is as follows: (a) 3.5 kHz, 90˚. (b) 6.75 kHz, 90˚. (c) 11.25 kHz, 90˚. (d) 11.75 kHz, 0˚. (e) 13 kHz, 30˚.

Figure 7 represents instantaneous pressure distribution patterns at the five peaks. Red indicates high positive pressure, and blue indicates high negative pressure. Thus, red and blue parts were the pressure anti-nodes with reverse phase.

At the first peak (3.5 kHz), only an anti-node developed in the cavity (Fig. 7 (a)). This pattern indicates that the primary resonance (the quarter wavelength resonance) occurred in the cavity. That is, the cavity resonated like a closed-open tube in the medio-lateral direction. At the second peak (6.75 kHz), two anti-nodes were observed at the upper and lower ends (Fig. 7 (b)). This indicates that the first mode of the closed-closed tube resonance (the half wavelength resonance) occurred in the supero-inferior direction, even though the cavity did not strictly form a closed-closed tube. At the third peak (11.25 kHz), three anti-nodes were observed. The middle anti-node had a reverse phase compared with the others. This indicates that the second mode of the closed-closed tube resonance (the one wavelength resonance) occurred in the supero-inferior direction. At the fourth peak (11.75 kHz), two anti-nodes were observed at the front and back ends (Fig. 7 (d)). This indicates that the first mode of the closed-closed tube resonance (the half wavelength resonance) occurred in the antero-posterior direction. At the fifth peak (13 kHz), four anti-nodes were observed (Fig. 7 (e)). This indicates that a two-dimensional resonance occurred in the cavity at that frequency.

HRTFs of modified models

First, we discuss the results of modification 1. Figure 8 represents HRTFs for the "2/3 height model." According to pressure distribution patterns, the first peak was caused by the first medio-lateral resonance, the second by the first supero-inferior resonance, the third by the first antero-posterior resonance and the fourth by the two-dimensional resonance. That is, because the cavity height was reduced, the frequency of the first supero-inferior resonance increased while the amplitude of the second supero-inferior resonance diminished beyond visibility. Also, the N1 like notch shifted to a higher frequency region, together with the second peak.

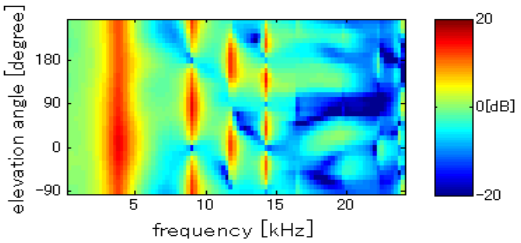

Figure 8. HRTFs for "2/3 height model."

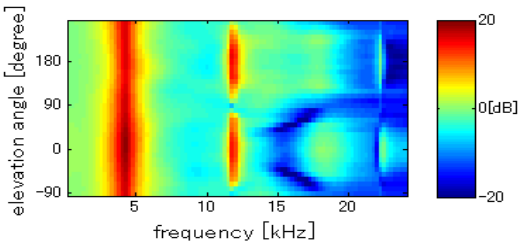

Figure 9. HRTFs for "1/2 height model."

Figure 9 represents HRTFs for the "1/2 height model." Only two peaks were observed. The lower one was caused by the first medio-lateral resonance, and the higher one by the first antero-posterior resonance. This modification removed not only the peaks derived from the supero-inferior resonances but also the N1 like notch. This fact indicates that the N1 like notch was associated with the supero-inferior resonances.

Next, we discuss the results of modification 2. Figure 10 represents HRTFs for the "1/3 position model." Although the peak-notch pattern for the "1/3 position model" was basically the same as that for "the primitive model", the amplitudes of peaks and notches differed between the two models. Especially, the amplitude of the second peak was considerably reduced. Figure 11 represents HRTFs for the "1/2 position model." In this modification, two peaks corresponding to the second and fifth peaks for the "primitive model" were lacking. At these two peaks, a pressure node was observed at the half height of the cavity (Fig. 7 (b) and (e)). For the "1/3 position model," therefore, the observation point came close to the node, and consequently the amplitude of the peak reduced. On the other hand, for the "1/2 position model," the observation point was placed on the node, and thus the peaks were lost. In other words, because the observation point was originally placed near the lower end of the cavity where a pressure anti-node existed, the first supero-inferior resonance appeared as the second peak. In addition, an N1 like notch was not observed in Fig. 11. This fact also indicates that this notch was associated with the supero-inferior resonance.

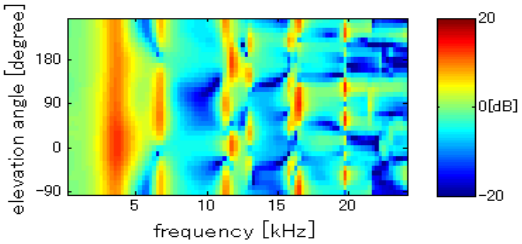

Figure 10. HRTFs for "1/3 position model."

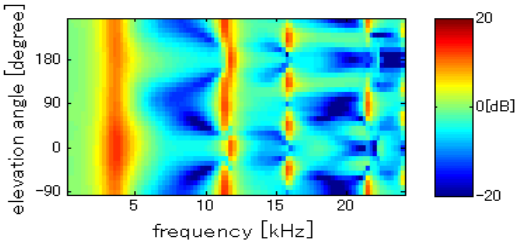

Figure 11. HRTFs for "1/2 position model."

Next, we discuss the results of modification 3. Figure 12 and 13 represent HRTFs for the "8 mm two-step model" and "4 mm two-step model," respectively. The peak-notch pattern of these models approached the typical pattern shown in Fig. 1 (b). The peak corresponding to P2 was clearly observed in Fig. 13. On the other hand, it was broad and ambiguous in Fig.12. This would be because the second peak was combined with the first one. The peak corresponding to P3 was observed at 11.5 kHz at narrow range of elevation angles centered at 90˚ in Fig. 13, while it was not clearly observed in Fig. 12. The notch corresponding to N1 appeared more clearly in Fig. 13. These results indicate that the geometry of the upper part of the cavity affected the amplitude and frequency of P2, P3, and N1.

Finally, we discuss the results of modification 4. Figure 14 represents HRTFs for the "three-step model." The typical peak-notch pattern as shown in Fig. 1 (b) was successfully obtained, although P3 was above 10 kHz. Compared to the "4 mm two-step model," the amplitude of the third peak increased, the notch pattern became clearer across a wider range of elevation angles, and the second peak became broad and appeared across a narrower range of elevation angles. For the "4 mm two-step model," the frequencies of the second and third peaks were 6.5 kHz and 11.5 kHz, respectively. For the "three-step model," they became 7.25 kHz and 11 kHz. Therefore, the second and third peaks converged for the "three-step model." These results also indicate that the geometry of the upper part of the cavity affected the amplitude and frequencies of P2, P3, and N1.

In order to obtain a peak-notch pattern much closer to the typical one shown in Fig. 1 (b) by removing the strong peak at 12 kHz and decreasing the third peak frequency, the "three-step model" was further modified. Because the peak at 12 kHz was caused by the first antero-posterior resonance, the cavity width (antero-posterior dimension) was reduced by 5 mm. Since the third peak was caused by the second supero-inferior resonance, each step was elongated by 3 mm. Figure 15 represents HRTFs for the modified "three-step model." As a result, the peak at 12 kHz was successfully removed, and the third peak shifted below 10 kHz. After the peak at 12 kHz disappeared, the second notch became visible below 0˚ and above 180˚. The frequencies of the first, second, and third peaks changed from 4.25 kHz, 7.25 kHz, and 11 kHz to 4.5 kHz, 7 kHz, and 9.75 kHz, respectively.

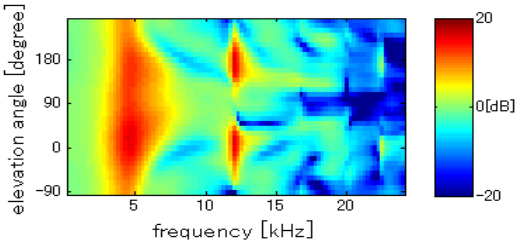

Figure 12. HRTFs for "8 mm two-step model."

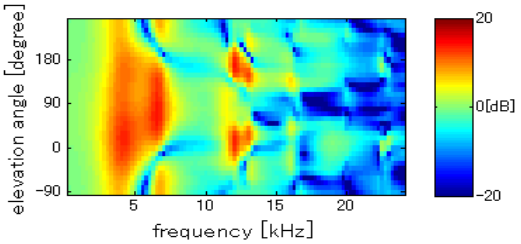

Figure 13. HRTFs for "4 mm two-step model."

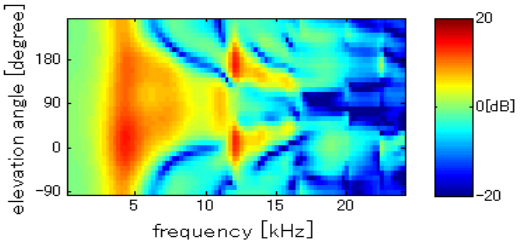

Figure 14. HRTFs for "three-step model."

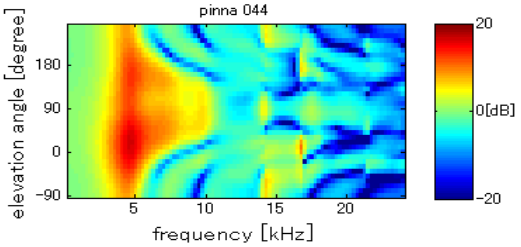

Figure 15. HRTFs for modified "three-step model."

Morphological features necessary for typical peak-notch pattern

In our preveous studies based on an MRI measured pinna, one, two, and three pressure anti-nodes were observed in the pinna cavities at P1, P2, and P3 frequencies, respectively [1-3]. Concering P1, Shaw and Teranishi reported that it was caused by the primary resonance of the concha [7]. Our previous studies [1-3] and the present study (Fig. 16 (a)) supported their result. Concering P2 and P3, however, the relationship among anti-nodes was unclear. In the present study, we clarified that P2 and P3 were caused by the first and second modes of the closed-closed tube resonances in the supero-inferior direction (Fig. 16 (b) and (c)). Furthermore, these resonances were associated with N1. Therefore, for generating the typical peak-notch pattern, morphologically essential features of the model's cavity are as follows:

(1) The pinna cavity has a certain depth.

(2) The pinna cavity is vertically long.

(3)The observation point is placed near the lower end of the pinna cavity.

(4)The depth of the pinna cavity decreases in the upper part.

The first feature relates to P1. As described above, since this peak was generated by the first resonance in the medio-lateral

direction (Fig. 16 (a)), the depth was the primary factor for the frequency. The second feature relates to P2, P3, and N1. Because the supero-inferior resonances generated P2 and P3 which coupled with N1, the vertical dimension was the primary factor for the resonances, while the geometry of the upper part of the cavity affected their amplitude and frequencies. According to the third feature, the observation point was placed on the pressure anti-node of the first and second supero-inferior resonances (Fig. 16 (b) and (c)). Thus, these resonances were included as P2 and P3 in HRTFs. The fourth feature affected the amplitude and frequency of P2 and P3, and contributed to generating a clear N1 pattern.

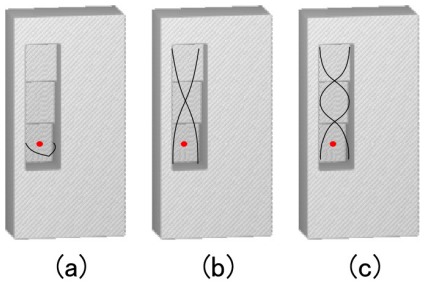

Figure 16. Pressure based resonance modes. (a) P1: the first closed-open resonance (1/4 wavelength resonance) in the medio-lateral direction. (b) P2: the first closed-closed resonance (1/2 wavelength resonance) in the supero-inferior direction. (c) P3: the second closed-closed resonance (1 wavelength resonance) in the supero-inferior direction.

Comparison between modeled and real pinnae

There are four major cavities on the human pinna: the concha, cymba, triangular fossa, and scaphoid fossa (Fig. 2). The lower, middle, and upper step of the "three-step model" would correspond to the concha, cymba, and triangular and scaphoid fossae, respectively. The concha is the deepest cavity, and thus it would determine P1 frequency. The pinna cavities are arranged vertically, and thus the whole shape of the pinna cavites is vertically long. Since the ear canal opens into the concha, the first order of the vertical resonance is observed as P2. The cymba, triangular and scaphoid fossae are shallower than the concha. Therefore, the four essential features for the typical peak-notch pattern discussed above are common in the human pinna.

While the elevation-dependent increase and decrease pattern of N1 frequency for the human pinna is usually symmetrical around approximately 120˚, that for the "three-step model" showed symmetry around 90˚. This would be because the long axis of the real pinna cavities is tilted at approximately 30˚ backward to the vertical axis. Because the lateral surface of the pinna faces slightly forward in the human body, the pinna model was tilted at 5˚ to the medial plane in the present study (Fig. 3 (c)). The effect was observed particularly in P1. The amplitude of P1 was the highest at 0˚ for all cases. This would be because the tilt of the pinna contributed to collecting the sound wave coming from the front direction.

CONCLUSION

In the present study, we developed simple pinna models and found that one of them, the "three-step model," generated a typical peak-notch pattern observed in the human HRTFs in the median plane. The analysis of the pressure distribution pattern revealed that peaks below 15 kHz had two different origins. Although P1 originated from the first closed-open resonance in the medio-lateral direction, P2 and P3 originated from the first and second closed-closed resonances in the supero-inferior direction. In addition, these vertical resonances brought about N1, although it was unclear what conditions would be necessary for generating the notch. The geometry of the upper and middle steps, corresponding to the upper cavities of the human pinna, affected the amplitude and frequency of P2, P3 and N1.

As a result of our analyses, four morphologically essential features necessary for the typical pattern were extracted: 1) the pinna cavity has a certain depth for P1; 2) the pinna cavity is vertically long for P2, P3, and N1; 3) the observation point is placed near the lower end of the pinna cavity for P2 and P3; and 4) the upper part of the pinna cavity reduces in depth for P2, P3, and N1. These features are commonly found in the human pinna.

REFERENCES

1 H. Takemoto, P. Mokhtari, H. Kato, R. Nishimura, and K. Iida, "Basic investigation for effects of pinna shapes on head related transfer functions," *Spring Proc. Meeting of the Acoustical Society of Japan*, 1445–1448 (2009) (in Japanese)

2 H. Takemoto, P. Mokhtari, H. Kato, R. Nishimura, and K. Iida, "Effects of individual difference of head shape on head related transfer functions," *Proc. Fall Meeting of the Acoustical Society of Japan*, 523–526 (2009) (in Japanese)

3 H. Takemoto, P. Mokhtari, H. Kato, R. Nishimura, and K. Iida. "Pressure distribution patterns on the pinna at spectral peak and notch frequencies of head-related transfer functions in the median plane," *e-Proc. the 1st International Workshop on the Principles and Applications of Spatial Hearing* (eISBN 978-981-4299-31-2), 4 pp. (2009)

4 K. Iida, M. Itho, A. Itagaki, and M. Morimoto, "Median plane localization using a parametric model of the head-related transfer function based on spectral cues," *Appl. Acoust.* **68,** 835–850 (2007)

5 H. Takemoto, P. Mokhtari, and T. Kitamura, "Acoustic analysis of the vocal tract during vowel production by finite-difference time-domain method," *J. Acoust. Soc. Am.* **123**, 3233, (2008)

6 P. Mokhtari, H. Takemoto, R. Nishimura, and H. Kato, "Efficient computation of HRTFs at any distance by FDTD simulation with near to far field transformation," *Proc. Fall Meeting of the Acoustical Society of Japan*, 611–614 (2008)

7 E. A. G. Shaw, and R. Teranishi, "Sound pressure generated in an external-ear replica and real human ears by a nearby point sources," *J. Acoust. Soc. Am*. **44**, 240-249, (1968)